Statistical Estimation of the Performance of a Fast-Neutron Multiplicity System for Nuclear Material Accountancy

David L. Chichester[a1], Scott J. Thompson[a], Mathew T. Kinlaw[a], James T. Johnson[a], Jennifer L. Dolan[b], Marek Flaska[b], and Sara A. Pozzi[b]

[a] Idaho National Laboratory, 2525 N. Fremont Avenue, Idaho Falls, Idaho, 83415, USA

[b] Department of Nuclear Engineering & Radiological Sciences, University of Michigan, 2355 Bonisteel Boulevard, Ann Arbor, Michigan 48109-2104, USA

Abstract

Statistical analyses have been performed to develop bounding estimates of the expected performance of a conceptual fast-neutron multiplicity system (FNMS) for assaying plutonium. The conceptual FNMS design includes 32 cubic liquid scintillator detectors, measuring 7.62 cm per side, configured into 4 stacked rings of 8 detectors each. Expected response characteristics for the individual FNMS detectors, as well as the response characteristics of the entire FNMS, were determined using Monte Carlo simulations based on prior validation experiments. The results from these simulations were then used to estimate the Pu assay capabilities of the FNMS in terms of counting time, assay mass, and assay mass variance, using assay mass variance as a figure of merit. The analysis results are compared against a commonly used thermal-neutron coincidence counter. The advantages of using a fast-neutron counting system versus a thermal-neutron counting system are significant. Most notably, the time required to perform an assay to an equivalent assay mass variance is greatly reduced with a fast-neutron system, by more than an order of magnitude compared with a thermal-neutron system, due to the reduced probability

[1] Corresponding author: email: david.chichester@inl.gov; phone: +1-208-526-8920

of random summing with the fast system. The improved FNMS performance is especially relevant for assays involving Pu masses of 10 g or more.

Keywords

Fast Neutron

Neutron multiplicity

Nuclear material accountancy

Safeguards

1 Introduction

The foundation of nuclear material accountancy is the determination of the mass of special nuclear material (SNM) – uranium and plutonium, and the use of this information to verify material inventory declarations. For bulk materials stored in containers one common method for doing this is to perform a paired set of measurements involving gamma-ray spectroscopy and time-correlated neutron emission analysis. The gamma-ray data is used to determine the isotopic content of the material, which is in turn used to help interpret the time-correlated neutron data and infer mass. The method is well understood and has been used for several decades.[1-5]

The approach is based on two characteristics of SNM. First is that, on average, the number of neutrons originating from fission, either spontaneous fission or induced-fission, is greater than one and that these emissions are correlated in time. The second characteristic is that in sub-critical assemblies of SNM one initial neutron can produce a series of subsequent fission events, and that neutrons generated in this process are also correlated in time. The fact that multiple neutrons are emitted from a single fission event is called multiplicity. The creation of multiple, connected instances of fission all correlated back to one initiating event, either spontaneous or induced fission, is called multiplication. The connected history of a

sequence of related fission events is called a fission chain. Careful observation and analysis of the distribution of the number of neutrons measured in a detector array within different-duration time windows, or conversely careful measurement of the time distribution of the waiting period in-between events, permits determination of a) the leakage multiplication rate of an SNM assembly and b) the total effective number of spontaneously-fissioning nuclei in the container. Combining this information with isotopic analysis determined using gamma-ray spectroscopy allows determination of the total amount of plutonium in the assembly.

Materials analyzed using time-correlated neutron counting may be presented for measurement in many forms. Examples include sealed canisters holding material at a storage vault, large cylinders holding solid uranium hexafluoride at an enrichment facility, and both fresh and irradiated nuclear fuel assemblies. Neutrons observed during measurements of these materials may be present due to many different sources. Some observed neutrons are naturally present as background radiation in the environment. Depending upon the material form and its purity, neutrons may be present as a result of nuclear reactions such as the interaction of energetic alpha particles with oxygen or other low-Z-nuclei where the alpha particle comes from the decay of an actinide. Importantly, when assaying plutonium, source neutrons may be present due to the presence of radioisotopes that decay by spontaneous fission with neutron emission. Regardless of the starting source, neutrons may also exist due to the creation of multi-generational chains of correlated fission events, through multiplication in the SNM. A listing of important nuclear data related to spontaneous fission for isotopes of uranium and plutonium is presented in Table 1.

Table 1 Spontaneous neutron emission rates for isotopes of uranium and plutonium.

Isotope	Half-life [6] [y]	Specific Activity [Bq kg^{-1}]	Spontaneous Fission (SF) Fraction of Decays [4,6]	Average SF Neutron Multiplicity, ν_{SF} [6,7] [n $fission^{-1}$]	Average Thermal Neutron Multiplicity, ν_T [8] [n $fission^{-1}$]	Average 2-MeV Neutron Multiplicity, $\nu_{2\text{-MeV}}$ [8] [n $fission^{-1}$]	SF Neutron Emission Rate [n s^{-1} kg^{-1}]
^{234}U	2.455×10^5	2.30×10^{11}	$(1.6 \pm 0.2) \times 10^{-11}$	1.81	2.36	2.63	6.67
^{235}U	7.038×10^8	7.80×10^7	$(7 \pm 2) \times 10^{-11}$	1.87	2.44	2.65	0.0105
^{236}U	2.342×10^7	2.39×10^9	$(9.4 \pm 0.4) \times 10^{-10}$	1.91	2.37	2.60	4.30
^{238}U	4.468×10^9	1.24×10^7	$(5.45 \pm 0.04) \times 10^{-7}$	2.01	2.49	2.53	13.7
^{238}Pu	87.7	6.34×10^{14}	$(1.85 \pm 0.05) \times 10^{-9}$	2.21	2.90	3.24	2.59×10^6
^{239}Pu	2.411×10^4	2.30×10^{12}	$(3.1 \pm 0.6) \times 10^{-12}$	2.16	2.88	3.18	15.4
^{240}Pu	6,561	8.40×10^{12}	$(5.70 \pm 0.2) \times 10^{-8}$	2.16	2.90	3.12	1.03×10^6
^{241}Pu	14.325	3.83×10^{15}	6×10^{-15}	2.25	2.95	3.21	50
^{242}Pu	3.750×10^5	1.46×10^{11}	$(5.49 \pm 0.09) \times 10^{-6}$	2.14	2.89	3.17	1.73×10^6

Note: The SF fraction of decay data for ^{241}Pu is not well known; uncertainty for this exceeds an order of magnitude, so too does the estimated SF neutron emission rate.

1.1 Need for Advanced Nuclear Material Assay Instruments

A large family of time-correlated neutron measurement systems has been produced for use in nuclear material accountancy. Traditionally, these systems used analog counting circuitry that included a series of coincidence gates and reported the number of occurrences of single, double, and sometimes also triple coincidence events within a user-selected time window. In contrast with these older systems, next-generation time-correlated neutron measurement systems digitally record all neutron events, assigning each event a record index corresponding to the relative time of each event in the detector subsystem; each event index is also often marked with the specific detector, or small subset of detectors, in the system in which it is registered. This data acquisition approach is often referred to as a "list-mode" system, it allows off-line post processing to analyze the data using multiple analytical approaches.

Systems that only report single and double neutron events are typically referred to as "coincidence counters" while those specifically designed for recording single, double, and higher-order coincidence

events are referred to as "multiplicity counters." A listing of several examples of these instruments is presented in Table 2, along with some of their key performance characteristics. These systems are typically comprised of large blocks of polyethylene forming an enclosure where a sample to be measured is placed, with inner cavities ranging in size from a few liters to several hundred liters. They use a couple dozen to over one hundred ^{3}He proportional counters embedded in the polyethylene walls of the instruments, to detect neutrons; they are usually in a cylindrically-symmetric layout.

Table 2 Deployed thermal-neutron coincidence and multiplicity assay instruments.

Instruments	Number of ^{3}He detectors	Neutron detection efficiency [%]	Die-away time [μs]	Description
Uranium Neutron Coincidence Counter (UNCL) [9]	24 (passive)/ 18 (active)	11.5/13.5	51	Designed for neutron coincidence measurements of uranium in standard fresh fuel assemblies, or plutonium in unirradiated mixed-oxide fuel assemblies. The active design uses an AmLi source.
Active Well Coincidence Counter (AWCC) [9]	42	33	51	Intended for assaying bulk quantities of HEU. The AWCC typically uses two matched AmLi sources, located in the top and bottom plugs of the cylindrical polyethylene housing.
High-Level Neutron Coincidence Counter (HLNCC) [9]	18	12	33	Developed for assaying plutonium. The HLNCC is specially designed for assaying large masses of plutonium, up to several kg, and for assaying Pu in a variety of forms.
In-Plant Pyrochemical Multiplicity Counter [4]	126	57	47	This counter was the first multiplicity system, rather than a doubles counter, designed for field use rather than laboratory use.
Plutonium Scrap Multiplicity Counter (PSMC) [4]	80	55	50	Designed for assaying impure plutonium, uranium and plutonium mixed oxides, and scrap materials over a wide mass range and over a high burn-up range.
High-Efficiency Neutron Counter (HENC) [4]	113	32	50	A system designed for assaying waste drums and intended to have a low limit of detection, to quantify small quantities of residual Pu.
Large Neutron Multiplicity Counter (LNMC) [4]	126	42	55	A large system specifically designed for assaying large drums, or plutonium storage containers. The system opens from the side to allow large items to be rolled in.
Epithermal Neutron Multiplicity Counter (ENMC) [10]	121	65	22	This counter is designed to assay impure Pu items, with high (α,n) neutron production, and to assay a large mass range of materials. It uses 10 atm ^{3}He tubes, in contrast with most of the other systems shown here, which use 4 atm tubes.

These instruments are reliable and they serve as workhorse nuclear material assay instruments in most facilities working with large quantities of SNM, especially plutonium. However, looking towards the

future, there are challenges regarding the continued use of these types of instruments. First and foremost, ^{3}He is no longer abundantly available, this shortage impacts the ability to purchase new assay systems that require ^{3}He tubes.[11] Second, while thermal- and epithermal-neutron counting systems are well suited for assaying pure Pu samples, and Pu samples with comparatively lower neutron emission rates, they are less useful for assaying samples with higher neutron emission rates. They are less suitable for higher-mass sample materials, impure Pu materials producing large numbers of uncorrelated neutron due to (α,n) reactions, or impure Pu materials containing non-trivial amounts of other spontaneously fissioning nuclei. As research progresses towards developing more advanced fuel cycles the necessity for assaying these types of materials will also grow.

1.2 Motivation for Using Fast Neutrons

Fast-neutron measurements have several potential advantages over thermal and epithermal neutron counters. The much shorter die-away times, $\mathcal{O}$(10 ns), associated with fast systems versus thermal or epithermal systems, $\mathcal{O}$ (10 μs), allow for measurements of higher-order multiplicity events with fewer random events, assays of samples with high uncorrelated (α,n) source terms, and rapid assays using active interrogation sources. Also, inspection times with fast neutron systems may be significantly reduced while maintaining acceptable measurement precision.

Employing thermal and/or epithermal neutron detectors for coincidence or multiplicity counting requires that the emitted neutrons be moderated prior to reaching a detector's active region. Reducing the average fission neutron energy (~2 MeV) to a level at which the necessary capture reaction has a greater probability eliminates the possibility to directly record correlated fission events. If an "optimal" counting gate width, G, is used (typically scaled by 1.26 times the detector die-away, G = ~1.26 τ), a thermal detection system with τ = 50 μs would have a gate width of ~63 μs.[4] Comparing this with a reasonable theoretical fast-neutron-based system (τ = 50 ns, G = 63 ns), the thermal system would be subject to three orders of magnitude more accidentals than would the fast die-away system. Further, a system that

operates on timescales comparable with the timescale of fission chain production also allows for the resolution of uncertainties in multiplication and detection efficiency.[12] An additional disadvantage of moderating neutrons prior to their detection is the initial energy information of the detected neutron is lost. With a scintillator-based system, or other fast-neutron-based system, at least some portion of the neutron's energy information is retained. By combining an energy discrimination capability with the aforementioned short counting gate width, items with elevated (α,n)-to-spontaneous fission ratios, α, can be assayed faster with a fast-neutron system; also, these systems can potentially improve the signal-to-background ratios for active interrogation assay measurements.[13]

1.3 Other Fast-Neutron-System Concepts

Early neutron-multiplicity work using liquid scintillators with pulse-shape discrimination (PSD) focused on basic science, studying multiplicity from heavy-ion fusion.[14] Similar instruments for related nuclear data measurements have been reported since then.[15] Examples of liquid scintillator-based fast-neutron assay systems specifically focused towards nuclear material accountancy have also been described in the literature.[16,17] These were motivated by difficulties associated with using the HLNCC for assaying impure plutonium. A semi-fast system was presented in 2001, where a borated-plastic scintillator was used for the neutron detector.[18] However, the neutron die-away time of this system, at 4 μs, was not fast enough to truly realize the advantages from fast-neutron measurements. Since then, modeling and simulation studies, along with some scoping experiments, have been reported for more capable, liquid-scintillator based assay instrument for nuclear safeguards.[19,20] Similar concepts have also been presented, including most recently a system focused towards assaying fresh fuel, using active neutron interrogation.[21-24]

For several years Idaho National Laboratory and the University of Michigan have been examining the use of fast-neutron multiplicity analysis as a method for assaying SNM for nuclear material accountancy.[25-

29] Primarily, this work has focused on passive measurements of plutonium but the use of active measurements aimed at assaying enriched uranium have also been explored.[30-31] This paper summarizes recent research activities focused towards designing and estimating the expected performance from a passive, scintillator-based fast-neutron assay system for safeguards assay measurements.[32]

2 FNMS Conceptual Design

The conceptual design for the FNMS consists of an array with thirty-two liquid scintillator cells arranged in a cylindrical layout surrounding an inner cavity with four levels, each having eight detectors. Model drawings of the arrangement are shown in Figure 1. The design uses commercially-available liquid scintillator detectors that have a 7.62 cm by 7.62 cm by 7.62 cm cubic volume of standard scintillating material, such as EJ-309.[23] In practice other scintillators, including pulse-shape discriminating plastics and stilbene could also be used. The detectors are positioned so that the photomultiplier tubes for the two inner-row detectors extend vertically between adjacent detectors in the upper and lower rings. This arrangement minimizes the footprint of the system, limiting it to an outer cylindrical volume with a diameter of approximately 45.2 cm and a height of approximately 57.6 cm. The sample cavity was designed to be identical in size to that of the HLNCC, with a diameter of 17 cm and a height of 41 cm. The FNMS sample cavity is shielded with lead to attenuate photons from materials placed in the cavity. For all calculations described in this paper the lead shielding had a thickness of 0.5 cm, but this can be increased to larger values if an application demands.

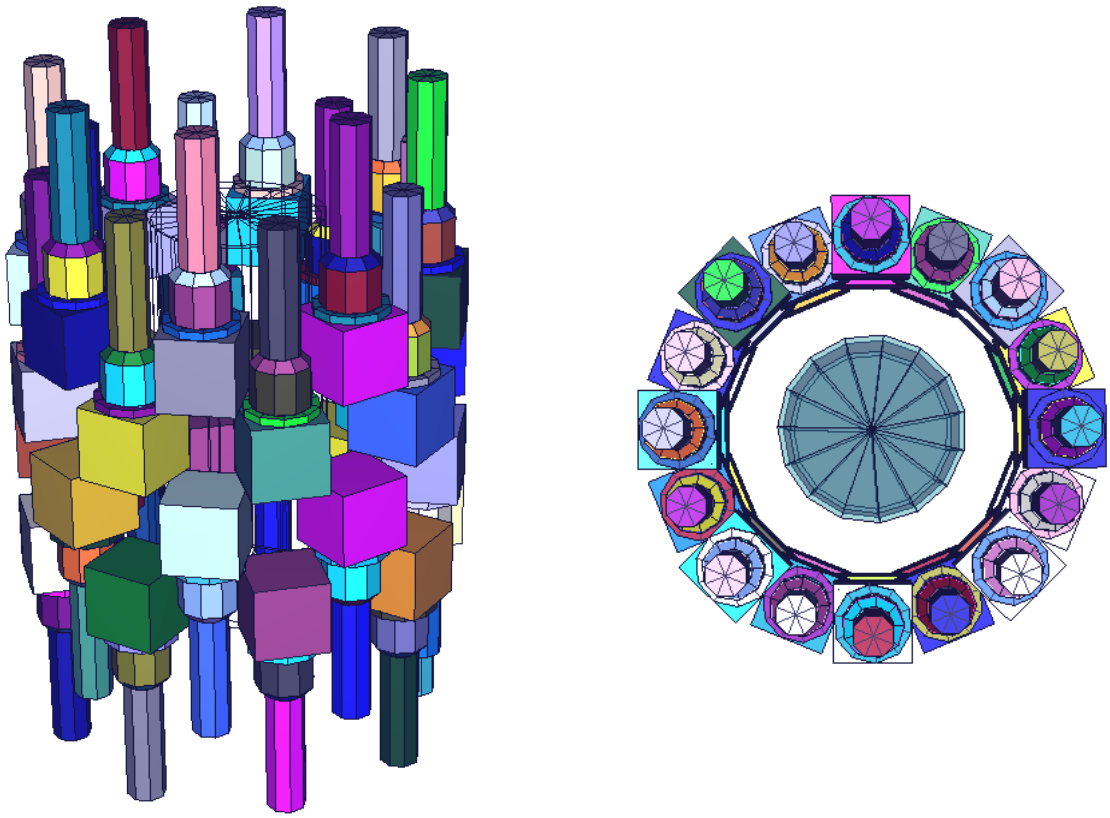

Figure 1 A side view (left) and top-down view (right) of the FNMS conceptual design, shown using the MCNPX Visual Editor.

3 Modeling the FNMS

Neutronic performance of the FNMS system was simulated using MCNPX version 2.7.0 and MCNPX-PoliMi version 2.7 to calculate several detection characteristics including the absolute neutron detection efficiency and the intrinsic neutron die-away constant.[33-35] Initial post-processing of these results was performed using MPPost, a software code distributed with MCNPX-PoliMi.[36] MPPost converts neutron scattering events occurring in the detector volume (inventoried in a MCNPX-PoliMi output file) and converts them light-pulse equivalent scalar based on the parameters of the detection system. To perform additional analyses a secondary post-processor analysis code was written to expand upon the MPPost. The enhanced post-processor took the MPPost methodology a step further, allowing for the

184 elimination of nearest-neighbor coincidences that occur from cross-talk in the detectors, which would be
185 done in practice for measured-data analysis.
186
187 A summary of the neutron detection efficiency calculations for the FNMC prototype is shown in Table 3.
188 These values are presented for neutron energies equivalent to that of a ^{252}Cf spontaneous fission emission
189 spectrum. It may be necessary to increase the pulse height detection threshold beyond the nominal 70
190 keVee value generally used for fast neutron measurements in order to achieve adequate pulse shape
191 discrimination when assaying samples with very high photon emission rates. Hence, efficiency values
192 were calculated for threshold levels of 70 keVee, 500 keVee, and 1.0 MeVee. In addition to general
193 detection efficiency, an appropriate time-dependent, die-away neutron spectrum was used to calculated
194 the system die-away constant; the fit for this resulted in an intrinsic neutron die-away constant of
195 approximately 5.9 ns.
196
197 **Table 3 Calculated absolute neutron detection efficiency values for the FNMS for several pulse**
198 **height detection thresholds.**

Pulse Height Threshold, keVee	Calculated Absolute Efficiency, %
70	9.3
500	1.6
1000	0.4

199
200
201 **4 Parametric study of Prototype FNMS performance**
202 To assess the potential performance capabilities of the prototype FNMS a set of parametric analyses were
203 performed to understand the impact of neutron detection efficiency, coincidence gate width, and die-away
204 time on the uncertainty associated with Pu mass determination. As a figure of merit (FOM) this analysis

used the relative standard deviation (RSD) for the determination of the effective ^{240}Pu mass, $^{240}Pu_{eff}$, of a sample as proposed by Ensslin et al.[37] Limits for this FOM are shown in Eq. 1, for low mass samples, and Eq. 2, for high mass samples.[38] Here τ is the system die-away time, ε is the system detection efficiency, t is the counting time, and m is the $^{240}Pu_{eff}$ mass. Ensslin's approach for analyzing neutron assay systems is not expected to produce exact values for as-built systems. However, it has been shown to produce good agreement, to within ~2-3, in many cases and it is well suited for use as a tool for comparing the relative performance of different system designs.

$$\boldsymbol{RSD} \propto \frac{1}{\boldsymbol{\varepsilon}\sqrt{\boldsymbol{m}\,\boldsymbol{t}}} \qquad \text{Eq. 1}$$

$$\boldsymbol{RSD} \propto \frac{\sqrt{\tau}}{\boldsymbol{\varepsilon}\,\sqrt{\boldsymbol{t}}} \qquad \text{Eq. 2}$$

Ultimately, the RSD is related to the ability to correctly determine the fission rate, F, in the sample and the associated uncertainty, σ_F. For low mass samples the primary factor impacting the RSD is the measurement uncertainty associated with triple counting, which degrades with decreasing mass. For high mass samples the primary factor impacting the RSD is the occurrence of accidental coincidence measurements, which increases nonlinearly with mass.[37] For this analysis the neutron background rate was assumed to be zero and system's pulse-shape-discrimination (PSD) capability for differentiating gamma-ray events from neutron events was assumed to be perfect. The high signal processing speed of fast-neutron measurements in the FNMS greatly reduces the impact of background radiation in the system. Our prior work has shown relatively fast-neutron coincidence measurements to be relatively immune to the very high background rates often associated with plutonium storage facilities.[29] This can be seen in the figures below by comparing the comparing the $\alpha = 0$ cases to the $\alpha = 2$ cases. For a real instrument the PSD performance, or gamma-ray rejection, is not zero; PSD rejection rates for these scintillators are generally in the range of 1 in 1000 or better for misclassifying photons as neutrons. To an extent this can be mitigated by adding lead shielding around the detector. However, in practice a more

functional mitigation method is to raise the energy cutoff threshold for considering counts. This reduces the system's detection efficiency, as shown in Table 3, but does eventually allow for the near total elimination of misclassified photons. Reducing the efficiency reduces the RSD values. Fortunately, for fast counting systems, the much lower die-away times with respect to thermal-neutron systems allows for some margin in this area. Two assay sub-scenarios were considered for three test cases, including $^{240}Pu_{eff}$ masses of 10,100, and 1000 g. These include an 'easy' scenario with a high leakage multiplication without alpha-induced neutron contributions and a more difficult scenario with no measureable leakage multiplication and a high alpha reaction rate.

The effects of absolute neutron detection efficiency upon the estimated mass assay variance are shown in Figure 2. In the figure M indicates the multiplication level for the sample and α indicates the fraction of the neutron events originating from (α,n) reactions (the uncorrelated fraction); one, five, and ten minute assay times were used. The mass uncertainty drops dramatically in all calculated scenarios up to approximately 10% efficiency. Between 10 and 30 percent the benefit of increased efficiency is less than a 50% decrease in variance for all instances shown. The upper-end efficiency value of 30% on this figure is a close approximation of 100% solid angle coverage using the scintillator detector components of the prototype design. System performance could be increased by the inclusion of additional detector rings to the design; however, the resulting improvement to solid angle coverage would not be substantial. Linear increases in the cost of hardware, electronics, and system size and weight would not have corresponding increases in detection efficiency, let alone performance. We believe the 9.3% absolute neutron efficiency achieved by the current prototype design (denoted by the vertical green line in the figure) to be close to an optimal configuration. In practice, depending upon the sample material, it might be necessary to raise the particle energy discrimination level to improve photon rejection. Raising the threshold from 70 keVee (assumed here) to 500 keVee, for example, would degrade the measurement precision by ~ 6× for these cases. However, for the ten minute analyses for example, the 100 g and 1,000 g sample uncertainties

would still be low (roughly of < 1% according to the FOM), while the 10 g uncertainty would only be slightly larger (roughly < 3% according to the FOM).

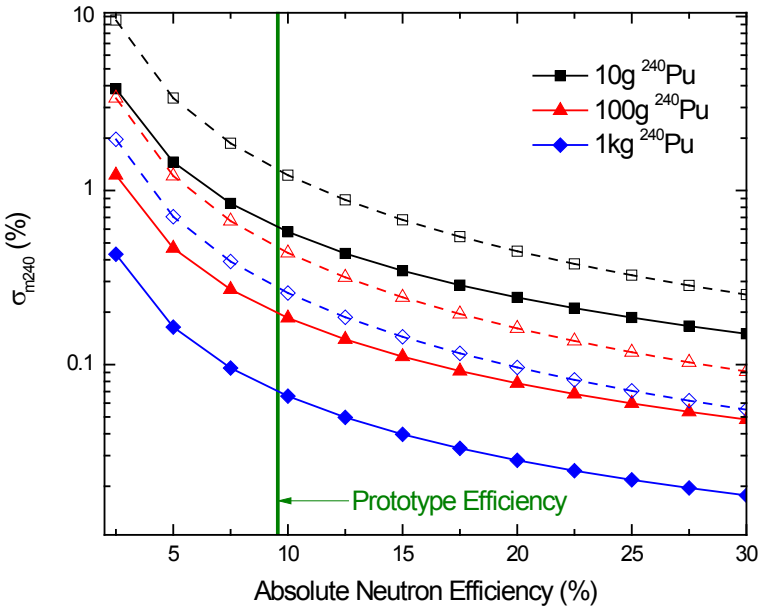

Figure 2 Assay variance for the prototype FNMS as a function of neutron detection efficiency. Values are provided for 60-s (blue, diamond), 300-s (red, triangle) and 600-s (black, square) measurement periods. High-multiplication low-alpha and low-multiplication high-alpha rate scenarios are shown by solid and dashed lines, respectively, in this figure and the following figures.

The analysis shows that the FNMS is relatively insensitive to changes in the gate width for values greater than 15 ns, as seen in Figure 3. The FNMS is somewhat sensitive to the die-away time in the region of the prototype system, as seen in Figure 4. However, this is a fixed constant of the system, based on geometry and material selection, and unlikely to change over time. Degradation of the precision is

observed to occur for the higher-mass, higher-α samples for increasing gate widths; this is due to the false recording of uncorrelated events as correlated events.

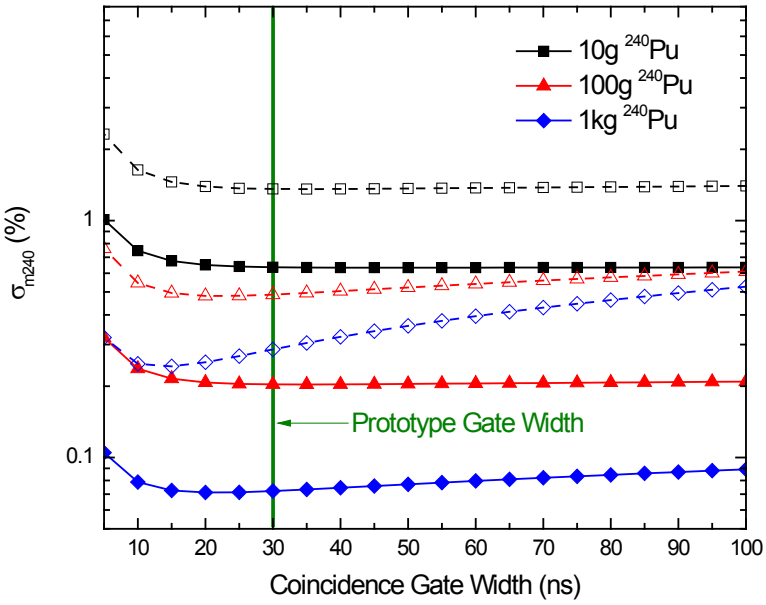

Figure 3 Assay variance for the prototype FNMS as a function of coincidence gate width. Values are provided for 60-s (blue diamonds), 300-s (red triangles) and 600-s (black squares) measurement periods.

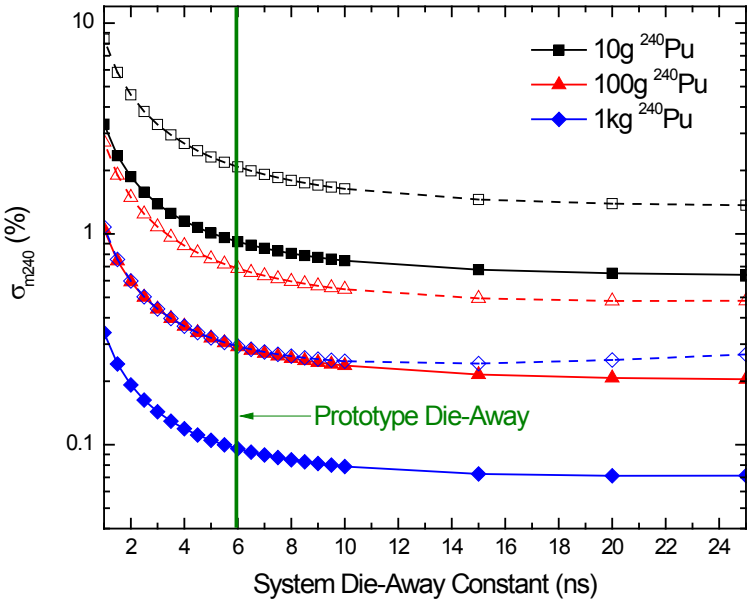

276

277 **Figure 4 Assay variance for the prototype FNMS as a function of detection system die-away.**

278 **Values are provided for 60-s (blue diamonds), 300-s (red triangles) and 600-s (black squares)**

279 **measurement periods.**

280

281 **5 Comparing the FNMS to the HLNCC**

282 To assess the expected performance of the FNMS in the context of nuclear material assay measurements,

283 an analytical comparison was made between the prototype FNMS and a commercial HLNCC (JCC-31,

284 Canberra Industries, Meriden, Conn.), again using RSD as the figure of merit. For this analysis the

285 HLNCC system parameters were taken from reference 37**Error! Bookmark not defined.**. A summary of

286 the parameters used in the calculations for both detection systems is shown in Table 4.

287

288

289

290

Table 4 System parameter values used for comparing the prototype FNMS and the HLNCC.

System Parameter	FNMS	HLNCC
Absolute Neutron Efficiency	9.3%	17.8%
Die-Away	5.9 ns	42 μs
Coincidence Gate Width	30 ns	64 μs
Gate Pre Delay	0 ns	4.5 μs

A comparison of the calculated assay variances as a function of time for the prototype FNMS and the HLNCC is shown in Figure 5. This figure demonstrates that a fast detector system has the ability to confirm mass assay values with much shorter measurement times than a comparably-sized thermal neutron-based system. After a 2.5 hour long assay, the prototype FNMS results have a predicted RSD variance approximately 2 orders of magnitude lower than that for the HLNCC. This figure also shows how the influence of the (α,n) reaction rate on mass variance is diminished with the faster system. Again, faster die-away allows for shorter coincidence windows, reducing the probability for false coincident neutron detections.

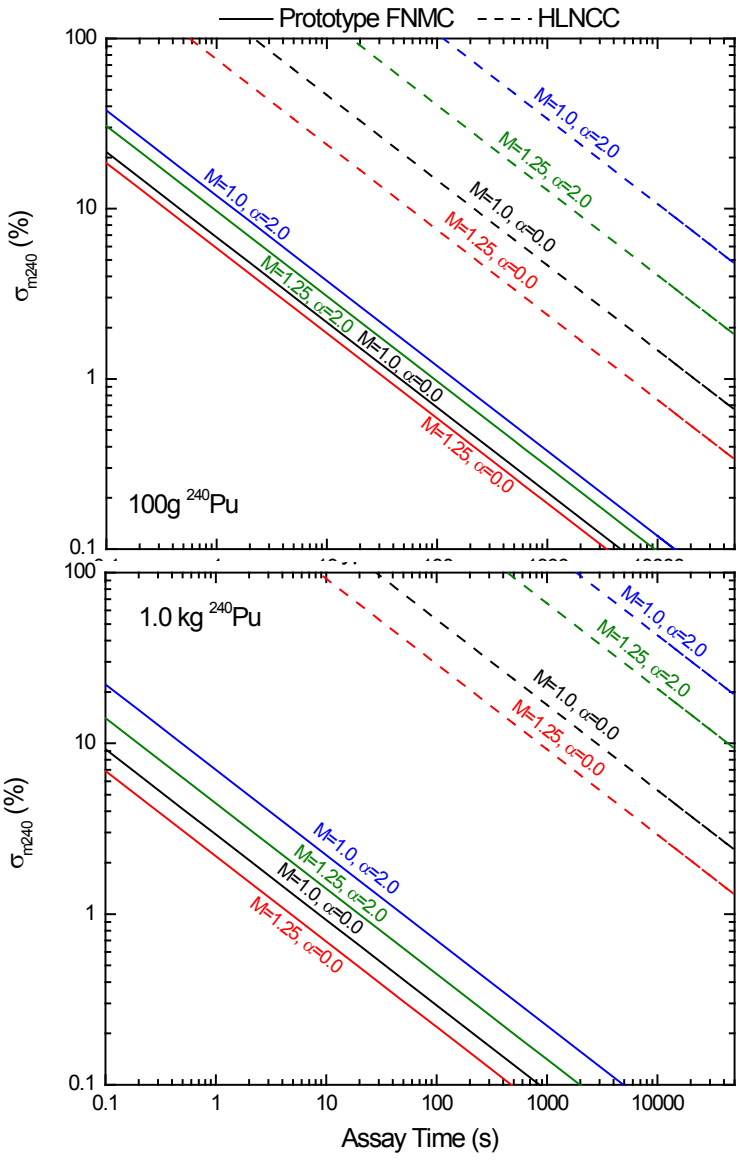

303

304 **Figure 5 Percent mass variance as a function of assay time for different measurement scenarios.**

305 **Values for the FNMS are represented with solid lines, while those for the HLNCC are shown with**

306 **dashed lines. Values are given for ^{240}Pu masses of 0.1 kg (top) and 1 kg (bottom).**

307

308 Similarly, plots of the prototype FNMS and the HLNCC RSD mass assay variances as a function of

309 $^{240}Pu_{eff}$ mass are presented in Figure 6. Data is shown for 1, 5, and 10 minute assay times. The overall

310 trend for the prototype system is that uncertainty continues to decrease exponentially with increasing

311 $^{240}Pu_{eff}$ mass before reaching a mass threshold where the benefits of elevated fission rates become
312 outweighed by high trigger rates and background contributions from alpha-induced neutron production
313 rates. For the high-alpha scenario in these plots (dashed lines) the mass threshold occurs around 1 kg of
314 $^{240}Pu_{eff}$ for the FNMS and nearly 1000 times lower for the HLNCC. This figure demonstrates that
315 extended assay times are needed for thermal neutron-based detection systems to achieve performance
316 levels comparable to fast system for mid- to high-mass assays.
317

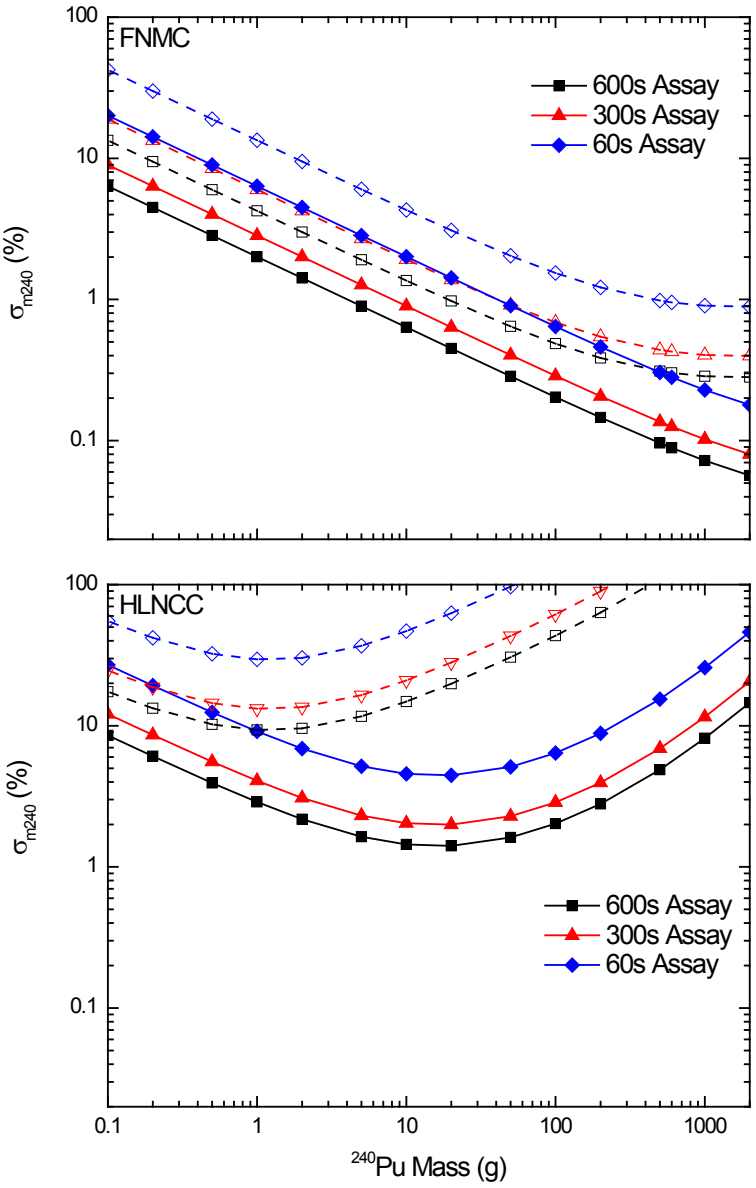

Figure 6 Assay variance for the prototype FNMS (top) and the HLNCC (bottom) as a function of ^{240}Pu mass. Values are provided for 60-s (blue diamonds), 300-s (red triangles) and 600-s (black squares) measurement periods.

6 Summary

Fast-neutron time-correlation analysis is a potentially useful method for assaying SNM for nuclear material accountancy. Fast counting systems have a high resilience to background effects and are far less likely to register false coincidences than slower, thermal-neutron based systems. As illustrated here, a practical fast-neutron system could be assembled having a similar floor-space footprint to traditional neutron coincidence counters employing ^{3}He proportional tubes, while having significantly improved performance in the coupled parameter space of counting time and precision. The performance of a conceptual FNMS layout having 32 detector cells was simulated and a simple analytical approach was used to compare it with a traditional thermal-neutron system, the HLNCC. The simulation and analytical analysis of the FNMS suggest that it has the potential to significantly reduce the counting times needed to achieve a particular measurement precision when compared with the HLNCC. Further, the FNMS appears likely capable to outperform traditional thermal-neutron based systems for assaying larger mass items, and items with high uncorrelated neutron emission source terms. Due to the short die-away time of the FNMS, this approach also appears well suited for use in active measurements for assaying uranium.

Further work is needed to assemble and evaluate a high-performance fast-neutron multiplicity system. Practical issues associated with the use of an FNMS under real conditions can only be identified through use and experimentation. One potential challenge likely to be encountered will be related to the potential for drift in the system response characteristics, such as effieciency, PSD performance, and uniformity, due to variability caused by temperature-induced drift in the system's components and electrical circuitry. Approaches for mitigating these effects might include, for example, the inclusion of a light pulser in the scintillator cells to monitor light yield, energy calibration, and timing, and making software-based corrections. Also, recent advances in nuclear instrumentation may substantially mitigate some of these challenges, most notably the use of solid-state photon sensors to replace traditional vacuum-tube photomultipliers.

Acknowledgments

This work was sponsored by the U.S. Department of Energy, Office of Nuclear Energy, Fuel Cycle Research and Development program. Support for one of the co-authors (JLD) was provided in part by the Nuclear Forensics Graduate Fellowship Program, which is sponsored by the U.S. Department of Homeland Security, Domestic Nuclear Detection Office and the U.S. Department of Defense, Defense Threat Reduction Agency. This manuscript has been authored by Battelle Energy Alliance, LLC under Contract No. DE-AC07-05ID14517 with the U.S. Department of Energy. The United States Government retains and the publisher, by accepting the article for publication, acknowledges that the United States Government retains a nonexclusive, paid-up, irrevocable, world-wide license to publish or reproduce the published form of this manuscript, or allow others to do so, for United States Government purposes.

1 Feynman, R. P., de Hoffmann, F., and Serber, R., "Dispersion of the Neuron Emission in U-235 Fission," J. Nucl. Energy 3 (1956) 64-69.

2 "Passive Nondestructive Assay of Nuclear Materials," Reilly, D., et al., eds., Report NUREG/CR-5550, US Nuclear Regulatory Commission, Washington, DC (1991).

3 Hage, W. and Cifarelli, D. M., "Correlation Analysis with Neutron Count Distribution for A Paralyzing Dead-Time Counter for the Assay of Spontaneous Fissioning Material," Nucl. Sci. Eng. 112 (1992) 136-158.

4 Ensslin, N., et al., "Application Guide to Neutron Multiplicity Counting," Report LA-13422-M, Los Alamos National Laboratory, Los Alamos, N.M. (1998).

5 Pazsit, I., Enqvist, A., and Pal, L., "A Note on the Multiplicity Expression in Nuclear Safeguards," Nucl. Inst. Meth. Phys. Res. A 603 (2009) 541-544.

6 Nichols, A. L., Aldama, D. L., and Verpelli, M., "Handbook of Nuclear Data for Safeguards: Database Extensions, August 2008," Report INDC(NDS)-0534, International Atomic Energy Agency, Vienna, Austria (2008)

7 Verbeke, J. M., Hagmann, C., and Wright, D., "Simulation of Neutron and Gamma Ray Emission from Fission and Photofission," Report UCRL-AR-228515, Lawrence Livermore National Laboratory, Livermore, Calif. (2010).

8 ENDF/B-VII.1 evaluated nuclear data library, retrieved from t2.lanl.gov/nis/data/endf/index.html, accessed March 6, 2014.

9 Kouzes, R. T., et al., "Introduction to Neutron Coincidence Counter Design Based on Boron-10," Report PNNL-21090, Pacific Northwest National Laboratory, Richland, Wash. (2012).

10 Pickrell, M. M., Veal, K., and Ensslin, N., "8. Fast and Epithermal Neutron Multiplicity Counters," Report LA-UR-07-1602, Los Alamos National Laboratory, Los Alamos, N.M. (2007).

11 Shea, D. A and Morgan, D., "The Helium-3 Shortage: Supply, Demand, and Options for Congress," Report R41419, Congressional Research Service, Washington, D. C. (2010).

12 McConchie, S., Hausladen, P., and Mihalczo, J., "Prompt Neutron Decay Constant from Feynman Variance Fitting," Proc. 50th Annual Meeting of the Inst. for Nucl. Materials Management, Tucson, Arizona, July (2009).

13 Miller, M. C., et al., "Design of a Fast Neutron Coincidence Counter," App. Rad. Iso. 48 (1997) 1549-1555.

14 Murakami, T., et al., "Performance of a Neutron Multiplicity Filter Composed of Six Liquid Scintillation Detectors," Nucl. Inst. Meth. Phys. Res. A 241 (1985) 172-176.

15 Dushin, V. N., et al., "Facility for Neutron Multiplicity Measurements in Fission," Nucl. Inst. Mth. Phys. Res. A 516 (2004) 539-553.

16 Hines, M. G., et al., "A Liquid Scintillator Neutron Coincidence Counter for Plutonium Assay," Nucl. Safeguards Tech. 2 (1986) 287-299.

17 Wachter, J. R., Adams, E. L., and Ensslin, N., "Prototype Fast Neutron Counter for the Assay of Impure Plutonium," Report LA-UR-87-3678, Los Alamos National Laboratory, Los Alamos, N.M. (1987).

18 Geist, W. H., et al., "Evaluation of a Fast Neutron Coincidence Counter for the Measurements of Uranium Samples," Nucl. Inst. Meth. Phys. Res. A 470 (2001) 590-599.

19 Frame, K. C., et al., "Neutron and Gamma Pulse Shape Discrimination in a Liquid Scintillator Counter for Neutron Multiplicity Measurements of Enriched Uranium," Report LA-UR-04-4868, Los Alamos National Laboratory, Los Alamos, N.M. (2004).

20 Frame, K., et al., "Development of a Liquid Scintillator Neutron Multiplicity Counter (LSMC)," Nucl. Inst. Meth. Phys. Res. A 579 (2007) 192-195.

21 Sheets, S. A., et al., "Comparison of Fast and Thermal Neutron Multiplicity Counters for Assaying Special Nuclear Materials," Proc. 51st Annual Meeting of the Inst. for Nucl. Materials Management, Baltimore, Maryland, July (2010).

22 Lavietes, A., et al., "Liquid Scintillator-Based Neutron Detector Development," IEEE Nucl. Sci. Symp. Conf. Rec. (2012) 230-245.

23 Tomanin, A., et al., "Design of a Liquid Scintillator-Based Prototype Neutron Coincidence Counter for Nuclear Safeguards," Proc. 54th Annual Meeting of the Inst. for Nucl. Materials Management, Palm Desert, Calif., July (2013).

24 Nakae, L. F., et al., "The Use of Fast Neutron Detection for Materials Accountability," Int. J. Mod. Phys: Conf. Series 27 (2014) 1460140.

25 Dolan, J. L., et al., "Measurement and Characterization of Nuclear Material at Idaho National Laboratory," J. Nucl. Mat. Manag. 38 (2009) 40.

26 Enqvist, A., et al., "A Combined Neutron and Gamma-Ray Multiplicity Counter Based on Liquid Scintillation Detectors," Nucl. Inst. Meth. Phys. Res. A 652 (2011) 48-51.

27 Kaplan, A. C., et al., "Validation of the MCNPX-PoliMi Code to Design a Fast-Neutron Multiplicity Counter," Proc. 53rd Annual Meeting, Inst. Nucl. Mat. Manag., Orlando, Fla., July 15-19 (2012).

28 Dolan, J. L., et al., "Passive Measurement of Organic-Scintillator Neutron Signatures for Nuclear Safeguards Applications," IEEE Nucl. Sci. Symp. Conf. Rec., Anaheim, Calif., Oct. 29 – Nov. 3 (2012) 203-206.

29 Dolan, J. L, et al., "Passive Measurement of Mixed-Oxide Fuel for Nuclear Nonproliferation," Nucl. Inst. Meth. Phys. Res. A 703 (2013) 102-108.

30 Dolan, J. L., et al., "Active-Interrogation Measurements of Induced-Fission Neutrons from Low-Enriched Uranium," Proc. 53rd Annual Meeting, Inst. Nucl. Mat. Manag., Orlando, Fla., July 15-19 (2012).

31 Dolan, J. L., et al., "Active-Interrogation Measurements of Fast Neutrons from Induced Fission in Low-Enriched Uranium," Nucl. Inst. Meth. Phys. Res. A 738 (2014) 99-105.

32 Chichester, D. L., et al., "MPACT Fast Neutron Multiplicity System Prototype Development," Report INL/EXT-13-30279, Idaho National Laboratory, Idaho Falls, Idaho (2013).

33 Pelowitz, D., "MCNPX User's Manual Version 2.7.0," Report LA-CP-11-00438, Los Alamos National Laboratory, Los Alamos, N.M. (2011).

34 Padovani, E., et al., "Introduction to MCNPX-PoliMi," University of Michigan, Ann Arbor, Mich. (2012).

35 Pozzi, S. A., "MCNPX-PoliMi for Nuclear Nonproliferation Applications," Nucl. Inst. Meth. Phys. Res. A 694 (2012) 119-125.

36 Miller, E. C., et al., "MCNPX-PoliMi Post-Processor (MPPost) Manual," University of Michigan, Ann Arbor, Mich. (2012).

37 Ensslin, N., Dytlewski, N., and Krick, M. S., "Assay Variance as a Figure of Merit for Neutron Multiplicity Counters," Nucl. Inst. Meth. Phys. Res. A 290 (1990) 197-207.

38 Pickrell, M. M., Veal, K., and Ensslin, N., "8. Fast and Epithermal Neutron Multiplicity Counters," Report LA-UR-07-1602, Los Alamos National Laboratory, Los Alamos, N.M. (2007).